IEEE Access
Multidisciplinary | Rapid Review | Open Access Journal

Received 18 August 2023, accepted 19 September 2023, date of publication 29 September 2023, date of current version 11 October 2023.

Digital Object Identifier 10.1109/ACCESS.2023.3320940

RESEARCH ARTICLE

# Autonomous Parking Path Tracking Control Based on Interference Suppression

**MAOFEI ZHU[1,2], QIAN LIU[1], JIANWEN ZHOU[3], WEI SHA[4], AND RUNXIN NIU[5]**
[1]School of Advanced Manufacturing Engineering, Hefei University, Hefei 230601, China
[2]Anhui Provincial Engineering Technology Research Center of Intelligent Vehicle Control and Integrated Design Technology, Hefei 230601, China
[3]China Automotive Engineering Research Institute Company Ltd., Chongqing 400039, China
[4]China PUJIN Intelligent Technology (Anqing) Company Ltd., Anqing 246501, China
[5]Hefei Institutes of Physical Science, Chinese Academy of Sciences, Anhui, Hefei 230031, China

Corresponding author: Jianwen Zhou (zhoujianwen@caeri.com.cn)

This work was supported in part by the University Natural Sciences Research Project of Anhui Province under Grant KJ2021A0988, in part by the Talent Research Fund Project of Hefei University under Grant 20RC06, in part by the National Key Research and Development Plan Project under Grant 2022YFD2001404-01, and in part by the Anhui Province Key Research and Development Plan Project under Grant 202304a05020065 and Grant 202304a05020018.

**ABSTRACT** Owing to the increased demand for autonomous driving and advanced driver assistant systems, autonomous parking configurations have been widely researched. In order to solve the problem of path tracking accuracy degradation, caused by ignoring the external interference in the actual parking process and the uncertainty of vehicle steering modeling, a parking path tracking algorithm, combining Sliding Model Control (SMC) and Extended State Observer (ESO), is proposed. First, the vehicle kinematics model is established, which includes many external interference factors, such as lateral position, speed, heading angle, uncertainty parameters and time delay of steering mechanism. Considering the vehicle physical constraints and boundary condition constraints, during the parking process, the parking reference path is designed according to reverse outbound driving, while the parking collision analysis and path smoothing are further carried out. Next, an ESO is designed to observe and compensate the external disturbances and model uncertainties, treating these as the total disturbances of the system. On this basis, a SMC for parallel parking path tracking is designed. The observed value of ESO is used as the compensation in the SMC, to weaken the influence of external interference. Finally, using Matlab simulation, the feasibility and effectiveness of the proposed path planning and tracking control method are verified. The simulation results show that, the maximum tracking error of lateral position is less than 0.01m, whereas the maximum tracking error of heading angle is less than 2.5°. Comparing two control strategies, the control effect of the designed SMC with ESO is better than that of the traditional SMC controller, while the ability of resisting external interference is stronger. In addition, real vehicle tests are carried out, to verify the effectiveness of the proposed control method. The test results show that, the vehicle can safely park in the parking space, quickly and accurately, even if there is external interference. The proposed method can produce the parking trajectory according to the given constraints and control the vehicle to complete the parking operation accurately along the planned path.

**INDEX TERMS** Autonomous parking, path tracking, extended state observer, interference suppression, sliding mode control.

## I. INTRODUCTION

The development of autonomous driving technology and the maturity of relevant intelligent algorithms lead to the rapid evolution of the autonomous parking technology. As the key technical link of autonomous driving technology, the

The associate editor coordinating the review of this manuscript and approving it for publication was Junho Hong.

autonomous parking system can not only solve the problem of parking difficulty, caused by the driver's in experience or the narrow space availability, but also improve the efficiency, safety and comfort of parking. Therefore, the research and development of autonomous parking systems are of fundamental practical importance [1]. An autonomous parking system includes environment perception, decision-planning, control execution and information interaction modules. Among them, the real-time, accuracy and reliability of parking path planning and tracking are the key to realizing autonomous parking [2].

The path planning module mainly uses the information obtained by the perception device or network, in order to make decisions and judgments. Parking path planning is about finding an optimal path from the starting point to the end point and is carried out based on the existing map. There are several methods to generate the path for the parking operation. An easy path planning method, based on a geometric approach, such as minimal turning radius, was proposed in prior art study [3]. However, this method shows good performance only in larger parking spots. Liang [4] used Bezier curves to smooth the trajectory, generated on multiple arcs on the circumference. Kim and Chung [5] applied a circular-linear curve, combined with vehicle obstacle avoidance constraints, to design a parking path. But the curvature discontinuity increased the difficulty of the vehicle path tracking. In order to generate a smooth and continuous parking path, Qian and Wu [6] proposed a piecewise Gauss pseudo spectral method, to solve the path planning problem indifferent parking spaces. The studies presented in [7], [8], and [9] adopted rapid exploration random tree approach, to generate the required local paths within the permitted driving area, while ensuring real-time performance in a dynamic environment. Furthermore, methods like reinforcement learning [10], special deep neural network [11], [12], midden Markov model [13], [14] are also widely used in path planning, exhibiting fast calculation speed and specific generalization ability, but requiring a large number of training samples to be collected.

The function of the tracking control module is to use an advanced algorithm to control the steering wheel, accelerator, brake and other actuators, so as to achieve driving, braking and steering, while maintaining the actual driving trajectory of the vehicle as consistent with the planned path as possible. In terms of trajectory tracking control algorithm, the autonomous parallel parking control method, based on fuzzy logic, proposed by Fang et al [15], can adapt to the fluctuation of speed. However, the confirmed fuzzy logical controller cannot park successfully, if the vehicle is outside the range of the effective position. Tu and Chen [16] established a parking feature model and control mode set, which determined the current feature state of vehicles, through pattern recognition. Next, the corresponding control mode was selected to control the vehicle parking path tracking function. The research in [17], [18], and [19] produced path tracking controllers based on feedback linearization control and sliding mode control, respectively. In [20] and [21], the presented path tracking control method, based on nonlinear model prediction, was applied to the path tracking of agricultural vehicles. Due to the short path and small space available for autonomous parking, the accuracy of path tracking determines the safety and reliability of the parking system. Hou and Dong [22] proposed an algorithm based on coordinates compensation, which further reduced the coordinates steady-state tracking error of the desired trajectory, by correcting the vehicle body angle online. In [23], a dynamic anti-saturation compensator is proposed, which can deal with the change amplitude and saturation velocity of system input, effectively reducing the tracking error of parking trajectory coordinates. In [24] and [25], the deviation between the expected trajectory and the feedback actual trajectory is analyzed, the interference of the steering system is considered, a non-time referenced sliding mode control and a quadratic optimal control scheme were designed to generate the target angle. The aforementioned control algorithms all induce a certain degree of improvement on the tracking accuracy of the parking path. However, considering the actual hardware circuit, the noise interference of various sensor signals can easily lead to large tracking error and low accuracy. The Kalman filter method exhibits the optimality of state estimation and reduces the disturbance of the system. In [26], a Dual Unscented Kalman Filter (DUKF) approach is proposed, where two UKFs run in parallel to simultaneously estimate vehicle state and parameters. In order to solve the problem of low accuracy in autonomous parking path tracking, caused by noise of various sensors, a parking path tracking algorithm, combining fuzzy control and Kalman filter, is proposed to reduce the measurement noise in vehicle position and course angle measurement data [27].

Based on the prior literature survey, most of the aforementioned trajectory tracking control methods need to establish an accurate mathematical model of the controlled object. However, the measurement noise of the sensor, the delay of the steering actuator, the disturbance caused by the road bumps and the ground obstacles interference with the parking system, create model uncertainty, and affect the tracking accuracy of the autonomous parking system. Therefore, how to eliminate the influence of external interference and the uncertainty of the kinematic model of the steering system and how to improve the tracking speed and accuracy of the autonomous parking operation, while enhancing the robustness of the system are the key problem of the autonomous parking control system. In this paper, the vehicle kinematics model with external interference is established, the path is planned using the elements of arc, straight line segment and arc, while the smooth parking path is fitted by quintic polynomial. An extended state observer is designed to observe and compensate the external disturbances and model uncertainties, treating these as the total disturbances of the system. On this basis, a sliding mode controller for parallel parking path tracking is designed. The observed value is used as the compensation in the sliding mode controller, to suppress the impact of external interference. The remainder of this paper is organized as follows. In Section II, the kinematics model of the parking system is established. In Section III, parallel parking reference path planning is provided. In Section IV, a sliding mode tracking control system with extended state observer is proposed. In Section V, the proposed tracking control system is simulated and verified. In Section VI, real vehicle tests are presented. Finally, conclusions are included in Section VII.

## II. VEHICLE KINEMATICS MODEL

In the process of autonomous parking, the driving speed of the vehicle is low, so its dynamic influence can be ignored, reasonably simplifying the vehicle kinematics model. The shape of the vehicle body is represented by a rectangle, while the vehicle kinematics model (Figure1) can be established.

Vehicle parameters are listed in Table 1.

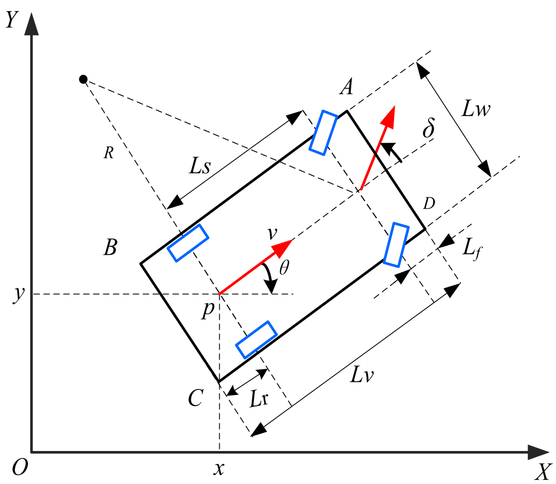


**FIGURE 1. Vehicle kinematics model.**

**TABLE 1. Vehicle parameters.**

| Parameters | Symbol | Value |
| --- | --- | --- |
| Vehicle length (mm) | $Lv$ | 4570 |
| Wheelbase (mm) | $Ls$ | 2700 |
| Vehicle width (mm) | $Lw$ | 1880 |
| Front overhang length (mm) | $L_f$ | 923 |
| Rear overhang length (mm) | $L_r$ | 947 |
| Maximum front wheel angle (°) | $\delta$ | 31.5 |

As shown in Figure1, the rear wheels of the vehicle are non steering wheels and $p$ is the center of the rear axle of the vehicle. The change of the coordinates of the center of the rear axle $p(x, y)$ represents the parking trajectory of the vehicle, $\theta$ is the heading angle, $\delta$ is the front wheel angle, $R$ is the steering radius, based on the center of the rear axle, and $v$ is the vehicle speed. In the actual parking process, the steering mechanism will exhibit time delay and modeling uncertainty, as well as external disturbances, such as road tire friction, which will cause deviation to speed fluctuation and heading angle. Considering the external interference and steering modeling uncertainty, the vehicle kinematics model equation is established as follows:

$$\begin{cases} \dot{x} = (v + \mathrm{v}^d)\cos\theta \\ \dot{y} = (v + \mathrm{v}^d)\sin\theta \\ \dot{\theta} = (v + \mathrm{v}^d)\cdot(\tan\delta + \delta^d)\Big/L_w \\ \dot{\delta} = (u - \delta)\big/T_d \end{cases} \tag{1}$$

where, $v^d$ represents velocity fluctuation disturbance, $\delta^d$ represents the disturbance of modeling uncertainty of the steering mechanism, $T_d$ indicates the steering delay time, $u$ is the front wheel steering control quantity.

By defining composite disturbance items, including lateral position disturbance $|d_1| \leq M$, heading angle disturbance, caused by steering uncertainty, $|d_2| \leq N$, where $M$ and $N$ are the maximum values of disturbance, the vehicle kinematics model in Eq. (1) can be written as follows:

$$\begin{cases} \dot{x} = v \cdot \cos\theta \\ \dot{y} = v \cdot \sin\theta + d_1 \\ \dot{\theta} = v \cdot \tan\delta\big/L_w + d_2 \\ \dot{\delta} = (u - \delta)\big/T_d \end{cases} \tag{2}$$

where, $d_1$ refers to the lateral position disturbance, measured in m/s; $d_2$ represents the heading angle disturbance measured in rad/s and caused by steering uncertainty.

According to the geometric relationship, the turning radius of the vehicle can be obtained as follows:

$$R = \frac{Ls}{\tan\delta} \tag{3}$$

According to the geometric relationship of the whole vehicle, the four vertex coordinates of the vehicle can be calculated. The left front vertex A coordinates:

$$\begin{cases} x_A = \mathrm{a} + (L_\mathrm{v} + L_f)\cos\theta - (L_\mathrm{s}\big/2)sin\theta \\ y_A = \mathrm{b} + (L_\mathrm{v} + L_f)\sin\theta + (L_\mathrm{s}\big/2)cos\theta \end{cases} \tag{4}$$

The left rear vertex B coordinates:

$$\begin{cases} x_B = x + (L_\mathrm{v} - L_r)\cos\theta - (L_\mathrm{s}\big/2)sin\theta \\ y_B = y + (L_\mathrm{v} - L_r)\sin\theta + (L_\mathrm{s}\big/2)cos\theta \end{cases} \tag{5}$$

The right rear vertex C coordinates:

$$\begin{cases} x_C = x + (L_\mathrm{v} - L_r)\cos\theta + (L_\mathrm{s}\big/2)sin\theta \\ y_C = y + (L_\mathrm{v} - L_r)\sin\theta - (L_\mathrm{s}\big/2)cos\theta \end{cases} \tag{6}$$

The right front vertex D coordinates:

$$\begin{cases} x_D = x + (L_\mathrm{v} + L_f)\cos\theta - (L_\mathrm{s}\big/2)sin\theta \\ y_D = y + (L_\mathrm{v} + L_f)\sin\theta + (L_\mathrm{s}\big/2)cos\theta \end{cases} \tag{7}$$

## III. PARALLEL PARKING REFERENCE PATH PLANNING

The parallel parking operation consists of three phases, as shown in Figure 2. First, the vehicle turns right, from point a at a radius $R_{ab}$ and drives to point b. Next, the steering wheel is turned back to its original position and the vehicle travels from point b to point c, along a straight line. Finally, the vehicle moves into the parking space from point c with the minimum turning radius $R_{cd}$. $O_{ab}$ and $O_{cd}$ are the steering center points of the first and the third phase of the parking process, respectively.

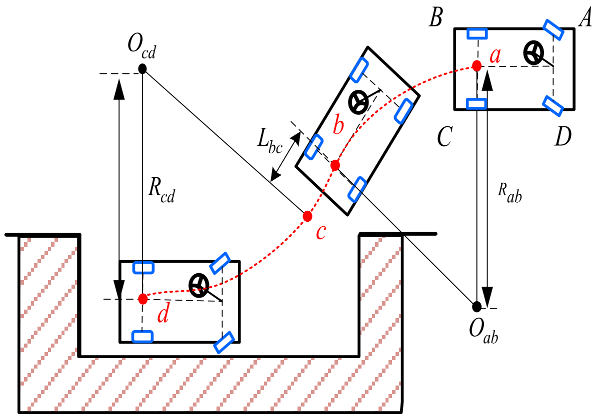


**FIGURE 2.** Parking process.

### A. COLLISION CONSTRAINT ANALYSIS OF CIRCULAR PATH IN PARKING SPACE

The parking route point is calculated by using the reverse outbound method, which is regarded as the process of driving out from point $d$ to point $a$ (Figure 2). The left rear position of the parking space is considered the origin point $O$, as shown in Figure 3, while the parking safety distance $L_t$ is set to 0.2m. The parking terminal point d coordinates can be obtained as follows:

$$(x_d, y_d) = (L_t + L_r, -0.5L_w) \tag{8}$$

Similarly, the coordinates of arc center $O_{cd}$ are also obtained as: $(L_t + L_r, R_{cd} - 0.5L_w)$.

During parking, the smaller the turning radius of the vehicle is, the smaller the risk of collision between the vehicle vertex D and the parking space point G is. Thus, the minimum parking space length $L_p$A is:

$$L_p = L_{OG} = 2L_t + L_{BD_0} \tag{9}$$

where, $L_{BD_0}$ refers to the distance between the left rear vertex B of the vehicle and the point $D_0$, which can be calculated by the following relation:

$$L_{BD_0} = \sqrt{\left(x_{D_0} - x_{O_{cd}}\right)^2 + \left(y_{D_0} - y_{O_{cd}}\right)^2 - (R_{cd} - 0.5L_w)^2} \tag{10}$$

When the vehicle reversely drives out of the parking space, the vehicle moves from point $d$ to point $c$, while the coordinates of point $c$ are obtained as:

$$(x_c, y_c) = (L_r + L_t + R_{cd}\cdot\sin\varphi, -0.5L_W + R_{cd}(1-\cos\varphi)) \tag{11}$$

where, $\varphi$ is calculated by the following relation:

$$\varphi = \arctan\left[\left(L_{BD_0} - L_r\right)/(R_{cd} - 0.5L_W)\right] - \arctan\left[\left(L_t + L_f\right)/(R_{cd} + 0.5L_W)\right] \tag{12}$$

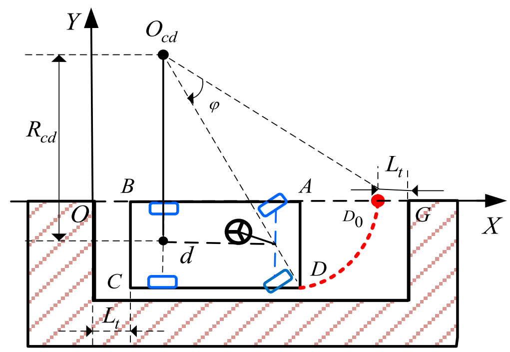


**FIGURE 3.** Vehicle right front vertex collision constraint.

### B. COLLISION CONSTRAINT ANALYSIS OF STRAIGHT PATH

As shown in Figure 4, the arc from point $a$ to point $b$ is tangent to the line segment connecting point $b$ to point $c$. According to geometric relations, the vehicle heading angle is equal to the center angle, corresponding to the turning arc of the vehicle. The slope of the line through points $b$ and $c$ is $\tan\varphi$. In order to ensure that the intersection of the extension line of the rear axle of the vehicle with the body and the parking space point $G$ do not collide, the distance $h$ between the parking starting point $a$ and the parking space needs to meet the following conditions.

$$h \geq R_{ab} - 0.5L_w - (R_{ab} - 0.5L_w)\cos\varphi \tag{13}$$

According to the geometric position relationship, the coordinates of point $b$ are obtained as follows:

$$(x_b, y_b) = (x_c + L_{bc}\cos\varphi, y_c + L_{bc}\sin\varphi) \tag{14}$$

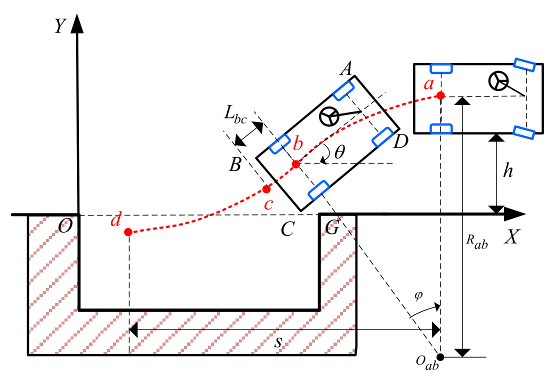


**FIGURE 4.** Straight right rear impact restraint.

Following, the constraint parameters to avoid collision are obtained as follows:

$$s = (R_{cd} + R_{ab}) \sin \varphi + L_2 \cos \varphi \tag{15}$$

$$h = (R_{cd} + R_{ab}) (1 - \cos \varphi) + L_{cd} \sin \varphi \tag{16}$$

In accordance with Eqs. (15) and (16), the length of the straight line segment between point $b$ and point $c$ is obtained as follows:

$$L_{bc} = h - (R_{cd} + R_{ab})\big/\sin \varphi \tag{17}$$

### C. COLLISION CONSTRAINT ANALYSIS OF OUTER CIRCULAR PATH OF PARKING SPACE

As shown in Figure 5, in order to ensure that the left front vertex A of the vehicle does not collide with the curb $A_0$, when the vehicle is driving along the arc $ab$, the minimum road width $L_d$ needs to meet the following conditions:

$$L_d \geq h + \sqrt{(R_{ab} + 0.5L_W)^2 + \left(L_S + L_f\right)^2} - R_{ab} - 0.5L_W \tag{18}$$

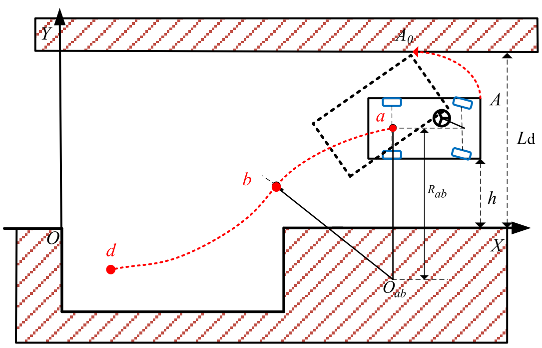


**FIGURE 5. Vehicle left front edge collision restraint.**

According to the geometric position relationship, the coordinates of $a$ can be derived as follows:

$$(x_a, y_a) = (x_b + R_{ab} \sin \varphi, y_b + R_{ab} (1 - \cos \varphi)) \tag{19}$$

### D. PATH SMOOTH FITTING

In the actual parking process, at the point where the arc is tangent to the straight line the steering needs to stop in order to turn instantaneously at a large angle. However, sudden sharp steering in situ will cause wear to the tires and the car steering mechanisms. In order to avoid this situation, the following quintic polynomial is used to optimize the path fitting.

$$y = g_5x^5 + g_4x^4 + g_3x^3 + g_2x^2 + g_1x + g_0 \tag{20}$$

where, $g_i(i = 0, 1, 2, 3, 4, 5)$ represent polynomial parameters. At parking start position $a$ and stop position $d$, the car body is parallel to the X axis, which means that the first derivative of the path equation Eq. (20) is 0. In addition, if the coordinates of four points $a, b, c, d$ are replaced into Eq.(20), polynomial coefficients and smooth path equations can be calculated.

## IV. PATH TRACKING CONTROLLER

In the autonomous parking control system, the measurement noise of the sensor, the disturbance caused by the road bumps and the ground obstacles cause external interference and model uncertainty, which affect the path tracking accuracy. In order to weaken the adverse effects of external interference, a path tracking controller is designed, based on vehicle kinematics, as shown in Figure 6.

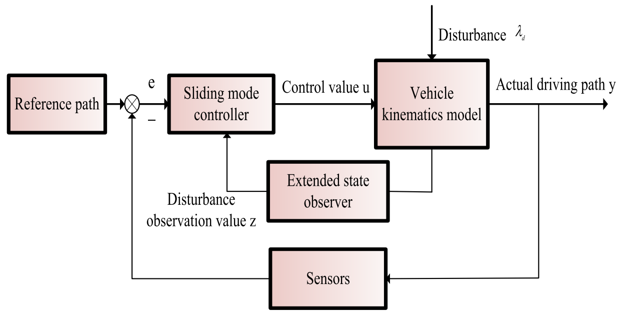


**FIGURE 6. Structure diagram of tracking control system.**

An extended state observer is designed to observe and compensate the external disturbances, as well as model uncertainties, such as representing the total disturbances of the system. On this basis, a sliding mode controller for parallel parking path tracking is designed. The observed value is used as the compensation in the sliding mode controller, to weaken the influence of external interference. The disturbance of the system is evidently estimated by the extended state observer and compensated in the sliding mode controller, to form a closed-loop control structure, so as to improve the tracking speed and accuracy of the autonomous parking system, while enhancing the robustness as well.

### A. EXTENDED STATE OBSERVER DESIGN

The extended state observer is the core part of Active Disturbance Rejection Control (ADRC) technology. It can observe and estimate the external disturbances in real time and compensate them in the controller [28]. In this paper, the external disturbance of the parking system and the modeling uncertainty of the steering system are regarded as the expanded state, whereas an expanded state observer is designed.

The parking path tracking model is regarded as a second-order system with respect to the longitudinal coordinate $y$ and heading angle $\theta$ of the target path. By defining state variable $x_1 = y$, the autonomous parking control system state equations can be derived from Eq.(2), as follows:

$$\begin{cases} x_1 = y \\ \dot{x}_1 = x_2 = v \cdot \sin\theta + d_1 \\ \dot{x}_2 = \dot{v} \cdot \sin\theta + \dot{d}_1 + v \cdot \cos\theta \cdot d_2 + v^2 \cdot \cos\theta \cdot \tan\delta \big/ L_s \\ \dot{x}_3 = \dot{v} \cdot \sin\theta + v \cdot \cos\theta \cdot d_2 + \dot{d}_1 \end{cases} \tag{21}$$

If $x_3$ is differentiable in Eq.(21), by defining $f = x_3$, the expanded system state equations are as follows:

$$\begin{cases} \dot{x_1} = x_2 \\ \dot{x_2} = x_3 + \dfrac{v^2 \cos\theta}{L_s} \tan\delta \\ \dot{x_3} = \dot{f} \\ y = x_1 \end{cases} \tag{22}$$

where, $f$ refers to the extended state variable. According to the Eq.(22), the following extended state observer is constructed to estimate the external interference of the autonomous parking system.

$$\begin{cases} e = z_1 - y \\ \dot{z_1} = z_2 - \beta_1 e \\ \dot{z_2} = z_3 - \beta_2 fal\left(e, \alpha_1, \eta\right) + \dfrac{v^2 \cos\theta}{L_s} u \\ \dot{z_3} = -\beta_3 fal\left(e, \alpha_2, \eta\right) \end{cases} \tag{23}$$

where, $e$ represents the error between the observed value and the actual output; $z_1 z_2$ and $z_3$ are the estimated values of the state value; $\beta_1$, $\beta_2$ and $\beta_3$ are error gain coefficients. The controller parameters are assumed to be univariate functions of loop gain bandwidth, thus the regulation process can be simplified [29]. Therefore, the relationship between controller coefficient $\beta$ and bandwidth $w_0$ is obtained as: $\beta_1 = 3w_0$, $\beta_2 = 3w_0^2, \beta_3 = w_0^3$; $\alpha_1 = 0.5, \alpha_2 = 0.25$ represent the nonlinear factor components of the following saturation function, reflecting the change rate of gain.

$$\begin{cases} fal\left(e, \alpha, \eta\right) = e \big/ \eta^{1-\alpha} \ |e| \leq \eta \\ fal\left(e, \alpha, \eta\right) = |e|^{\alpha}\, sgn\left(e\right) |e| > \eta \end{cases} \tag{24}$$

where, $fal\left(.\right)$ refers to saturation function, which is used to control signal chattering; $\eta$ is the control parameter of saturation function and its value is set to 0.01.

### *B. DESIGN OF SLIDING MODE TRACKING CONTROLLER*

The sliding mode controller is designed with characteristics of less adjustable parameters, fast response speed and simple physical implementation. By designing an appropriate sliding mode surface and control law, the system state trajectory can quickly reach the sliding mode surface and converge to a stable state. In this paper, the aforementioned observed value is used as the compensation in the sliding mode controller, to weaken the influence of external interference. The controlled object model of the autonomous parking system is described in Eq. (2), while the error $e = y - y_r$, which leads to the sliding surface function being designed as follows:

$$s = \mathrm{k}_1 e + \dot{e} \tag{25}$$

where, $\mathrm{k}_1$ refers to the gain parameter of the error. The following formula is obtained by differentiating the sliding surface function.

$$\dot{s} = k_1 \dot{e} + \dot{v} \cdot \sin\theta + v \cdot \cos\theta \cdot d_2 + v^2 \cdot \cos\theta \cdot \tan\delta \Big/ L_s - \ddot{y_r} + \dot{d_1} \tag{26}$$

By simplifying Eq. (26), the following relation is obtained.

$$\dot{s} = k_1 \dot{e} + f + \frac{v^2 \cos\theta}{L_s} \tan\delta - \ddot{y_r} \tag{27}$$

The exponential approach law is chosen to improve the quality of sliding mode approach motion.

$$\dot{s} = -k_2 - k_3 sgn\left(s\right) \tag{28}$$

where, $\mathrm{k}_2, \mathrm{k}_3$ represent the parameters of approach law; $sgn\left(.\right)$ is a symbolic function. A Lyapunov Function is designed as: $\lambda = 0.5s^2$, while the derivative of $\lambda$ is obtained as:

$$\dot{\lambda} = s\dot{s} = -k_2 s^2 - sgn\left(s\right) s \leq 0 \tag{29}$$

Only when $s = 0$, there is $\dot{\lambda} = 0$. Therefore, $s$ keeps approaching 0, that is, $s$ is stable on the sliding mode surface of $s = 0$, whereas the system tracking error converges to a stable state, under the sliding mode design of the reaching law with external interference. The control value $u$ of the sliding mode controller can be obtained by combining the Eqs.(27) and (28).

$$u = \frac{L_s}{v^2 \cos\theta} \left( \dot{y_r} - f - k_1 \dot{e} - k_2 s - k_3 sgn\left(s\right) \right) \tag{30}$$

where, $f$ refers to the extended state, which can be estimated by the extended state observer in Eq. (23). In order to suppress the chattering phenomenon and ensure the smooth switching surface of the system, the sign function $sgn\left(.\right)$ in Eq. (30) is replaced by the following saturation function.

$$sat(s/\varepsilon) = \begin{cases} 1 s \geq \varepsilon \\ s \big/ \varepsilon \ |s| < \varepsilon \\ -1 s \leq -\varepsilon \end{cases} \tag{31}$$

Finally, accurate tracking control is realized by adjusting the values of $\mathrm{k}_1$, $\mathrm{k}_2$ and $\mathrm{k}_3$ parameters.

## V. SIMULATION ANALYSIS

### *A. PATH PLANNING SIMULATION*

In order to verify the effectiveness of path planning, a simulation model is established in MATLAB. Using the vehicle parameters, as listed in Table1, the minimum turning radius is $R_{ab} = 4.35$m, $R_{cd} = 4.35$m, and the road width is $L_d = 3.9\ m$. The parameter h is selected as 1.28 m, 1.66 m and 2.15 m, based on the minimum longitudinal distance, average distance and maximum longitudinal distance between the right side of the vehicle body and the corner of the parking space, respectively. The simulation result is shown in Figure 7, where the driving track of the center of the rear axle of the vehicle is illustrated. It is thus clear that, parking paths can be calculated even at different starting points,

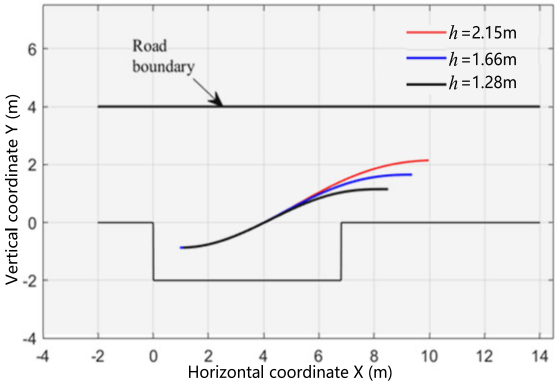


**FIGURE 7. Path planning.**

which shows the good adaptability and robustness of the path planning approach.

The distance between the vehicle vertex D and the parking corner G, during parking, is shown in Figure 8. It can be seen that, the vehicle will not collide with the parking space boundaries, when driving along the planned path.

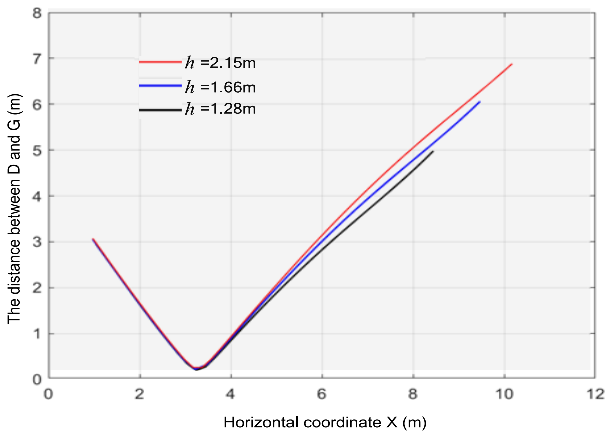


**FIGURE 8. Distance between the vehicle vertex D and the parking corner G in three driving path cases.**

### B. PATH TRACKING CONTROL SIMULATION

The effectiveness of the path tracking control algorithm for autonomous parking system is verified in Matlab / Simulink environment. In order to reflect the real parking scene, the parking speed is set as $v = 1\text{m/s}$. Considering the influence of external disturbances on the autonomous parking system, the following interference are set to apply to the system.

$$\begin{cases} d_1 = 0.01\sin(\pi t) + 0.01\cos(3t) \\ d_2 = 0.03\sin(5t) \end{cases} \tag{32}$$

The parameter h is selected as 1.28 m, indicating actual narrow parking space scene. Therefore, the path in this scenario is selected as the reference path in this simulation. In order to verify the tracking performance, the traditional sliding mode control without observer is selected as benchmark to compare to the designed extended state observation sliding mode controller. The parameters $k_1$, $k_2$ and $k_3$ of the traditional SMC are set to 42, 9 and 0.2, while ESO parameters $w_0$, $k_1$, $k_2$, $k_3$, $\varepsilon$ of SMC are set to 10,2, 5,0.01 and 0.5, respectively. The coefficient of reference path $g_5 = 3.8203 \times 10^{-4}$, $g_4 = -0.0073$, $g_3 = 0.034$, $g_2 = 0.0518$, $g_1 = -0.1339$, $g_0 = -0.6556$.

The comparison of the tracking performance curves of the two controllers is shown in Figure 9. In the case of external disturbance, the traditional SMC shows chattering and large tracking deviation. However, the path of the SMC with ESO is basically consistent with the reference path, whereas the tracking error is small.

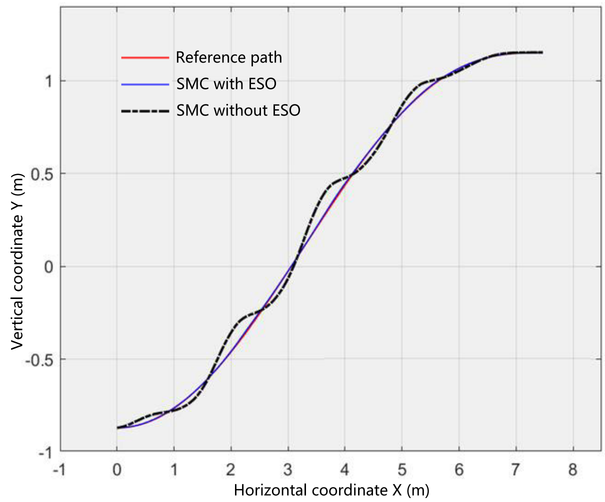


**FIGURE 9. Performance comparison of path tracking approaches.**

In the simulation, the external complex disturbance to the system, observed by the designed ESO, is shown in Figure 10. It can be seen that, the composite estimation value of the heading angle disturbance, caused by the lateral position disturbance and steering uncertainty, caused by the extended

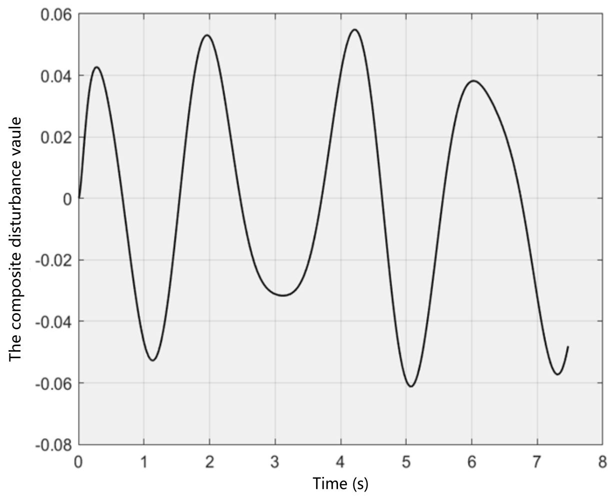


**FIGURE 10. System disturbance estimator.**

state observer, is basically consistent with the amplitude and fluctuation frequency trend of the disturbance value, applied by the simulation, indicating that compensating the disturbance estimation value of the observer in the controller can improve the tracking accuracy.

The vehicle lateral position tracking error, during parking, is shown in Figure 11. In case of external disturbance, the maximum lateral position tracking error of SMC with ESO is 0.01m, while the average tracking error is about 0.003m. However, for SMC controller without ESO, the maximum tracking error is 0.07m, while the average error is 0.034m. The vehicle heading angle tracking curves of the two controllers are shown in Figure 12. The heading angle tracking error of SMC without ESO is large, reaching a maximum value of 9 °. In contrast, the maximum tracking error of SMC with ESO in heading angle is only 2.5 °. The designed SMC with ESO path tracking controller has significantly improved the control effect, the tracking control accuracy and reduced the stability error, which proves the effectiveness of the proposed algorithm.

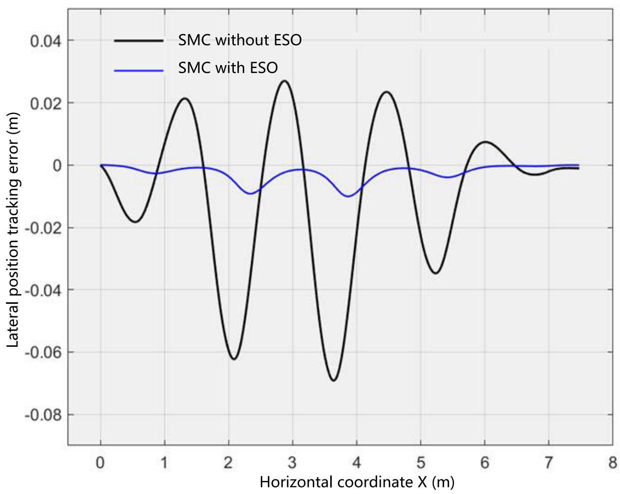


**FIGURE 11.** Lateral position tracking error.

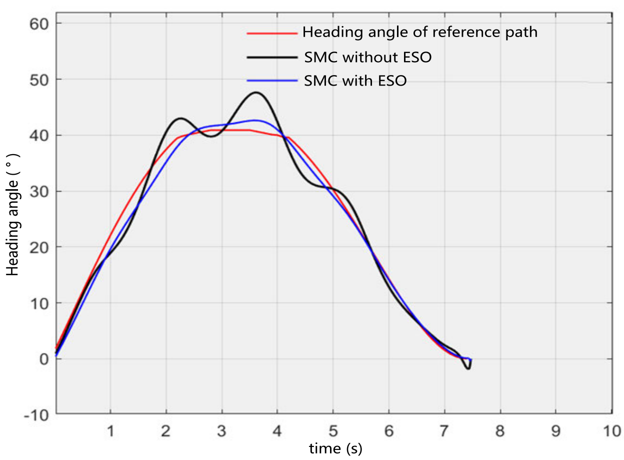


**FIGURE 12.** Vehicle heading angle tracking curves.

## VI. REAL VEHICLE TEST VERIFICATION

### A. TEST PLATFORM

In order to verify the effectiveness of the designed control strategy on the actual vehicle, a test with a real vehicle is carried out. The instrument used in the test and the schematic of the test are shown in Figure 13.


**FIGURE 13.** Real vehicle test system.

The autonomous parking control system of the execution parts of the test vehicle was reformed by wire control, including steering system, braking system, power system and gear system, which respectively realized the control functions of active steering, velocity tracking and motion direction control, so that the lateral and longitudinal movement of the test vehicle could be directly controlled by signals on a CAN bus. The steering wheel angle signal is provided by the angle sensor of the electric power steering system, while the wheel speed pulse signal and longitudinal acceleration signal are provided by the wheel speed sensor and the acceleration sensor of the braking system, respectively. The test vehicle is equipped with twelve ultrasonic radars, of which four are short-range mode radars attached at the front and rear, while two are long-range mode radars positioned at the left and right sides. In addition, a surround view camera is installed at the front, rear, left and right of the test vehicle. The fusion of data from the ultrasonic radar and the around view camera can realize the detection of space parking spaces and crossed parking spaces. The autonomous parking controller processes the aforementioned signals and parking space information, to obtain the target parking trajectory information and control variables, including target steering angle, target velocity and target gear, while it sends the target control signal to each executive control system. The above algorithm is converted into C code through MATLAB modeling and uploaded to the autonomous parking controller. The signal communication between each system is carried out through the CAN bus.

### B. TEST RESULTS AND ANALYSIS

The parameters of the autonomous parking test are listed in Table 1. A parallel parking space with a length of 6.6m and a width of 2.2m is detected by the ultrasonic radar and the all-around view camera.

Figure 14 illustrates the vehicle driving track, as recorded during the process of autonomous parking. It can be seen that, the SMC with ESO exhibits good control performance and the derived driving path is relatively smooth. In particular, the straight line segment section basically coincides with the reference path.

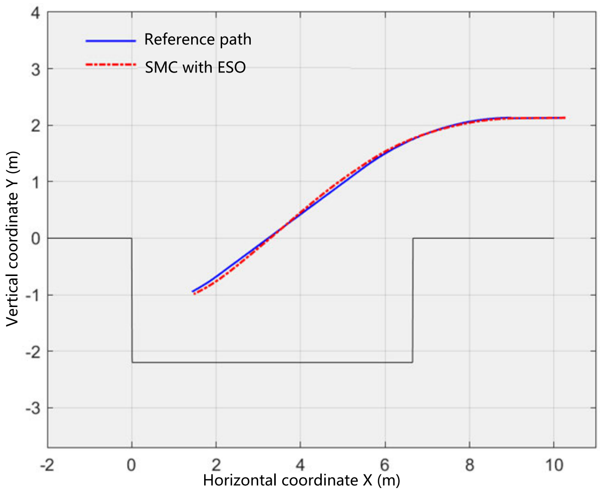


**FIGURE 14. Vehicle driving path.**

During parking, the test vehicle runs at the expected speed of 5km/h, producing a lateral tracking error, as shown in Figure 15. The maximum lateral tracking deviation occurs when the steering wheel is turned quickly twice, during parking. The maximum lateral tracking error is 0.065m and the average error is 0.04m. The actual driving speed curve of the vehicle, during parking, is shown in Figure 16. The state observer is designed to predict the external disturbance and compensate it in the sliding mode controller, so the speed fluctuation will not have a significant impact on the path tracking accuracy, thus reflecting the high robustness of the controller.

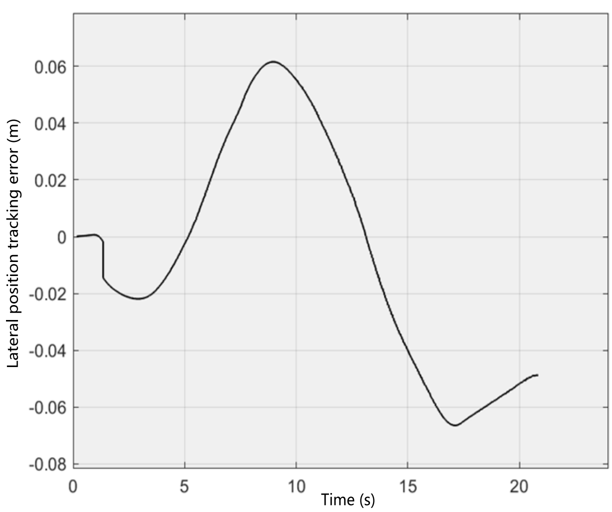


**FIGURE 15. Lateral position tracking error.**

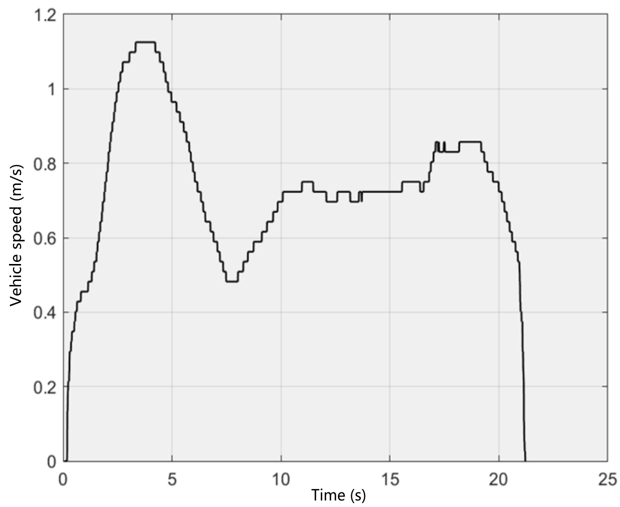


**FIGURE 16. Vehicle actual driving speed curve.**

The real vehicle test heading angle is shown in Figure 17, where the maximum deviation is 4.5°. The real vehicle test shows that, the SMC with ESO can realize the autonomous parking process with uncertain external disturbance, at low speed without collision, while the tracking control accuracy and robustness are better.

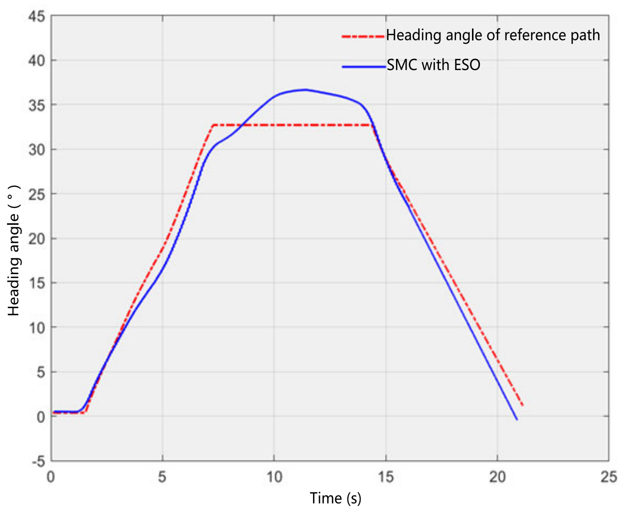


**FIGURE 17. Vehicle heading angle curve.**

## VII. CONCLUSION

1) This paper proposes a parking path tracking algorithm, which combines sliding model control and extended state observer, to solve the problem of path tracking accuracy degradation, caused by ignoring the external interference in the actual parking process and the uncertainty of vehicle steering modeling. By analyzing the parking movement process, the vehicle kinematics model with external interference is established. It includes lateral position, speed, heading

angle, uncertainty parameters and time delay of the steering mechanism.

2) In the planning module, by establishing the vehicle kinematics model, physical system constraints, boundary constraints and obstacle avoidance constraints, the parking reference path is designed according to the notion of reverse outbound driving, composed of three path segments: arc, straight line and arc, while the parking collision analysis is carried out in each one, respectively. The reference path is further smoothly fitted using a quintic polynomial. An ESO is designed to observe and compensate the external disturbances and model uncertainties, treated as the total disturbances of the system. On this basis, a SMC for parallel parking path tracking is designed. The observed value of ESO is used as the compensation in the SMC to weaken the influence of external interference.

3) Through simulation and real vehicle testing, the feasibility and effectiveness of the proposed path planning and tracking control method are verified. The results show that, the control effect of the designed SMC with ESO is better than that of the traditional SMC controller, while the ability of resisting external interference is stronger. The proposed method can plan the parking trajectory according to the constraints and control the vehicle to park in the parking space safely, quickly and accurately, even if there is external interference. However, this method still has some shortcomings, since it requires a large amount of computation. Reducing the error and improving the computational efficiency would be part of future research.

## REFERENCES

[1] D. Qiu, D. Qiu, B. Wu, M. Gu, and M. Zhu, "Hierarchical control of trajectory planning and trajectory tracking for autonomous parallel parking," *IEEE Access*, vol. 9, pp. 94845–94861, 2021, doi: 10.1109/ACCESS.2021.3093930.

[2] Z. Qin, X. Chen, M. Hu, L. Chen, and J. Fan, "A novel path planning methodology for Automated Valet Parking based on directional graph search and geometry curve," *Robot. Auton. Syst.*, vol. 132, Oct. 2020, Art. no. 103606, doi: 10.1016/j.robot.2020.103606.

[3] S. Choi, C. Boussard, and B. d'Andréa-Novel, "Easy path planning and robust control for automatic parallel parking," in *Proc. 18th IFAC World Congr.*, Milano, Italy, vol. 44, Aug. 2011, pp. 656–661.

[4] Z. Liang, G. Zheng, and J. Li, "Automatic parking path optimization based on Bezier curve fitting," in *Proc. IEEE Int. Conf. Autom. Logistics*, Zhengzhou, China, Aug. 2012, pp. 583–587.

[5] D. Kim, W. Chung, and S. Park, "Practical motion planning for car-parking control in narrow environment," *IET Control Theory Appl.*, vol. 4, no. 1, pp. 129–139, Jan. 2010, doi: 10.1049/iet-cta.2008.0380.

[6] L. Qian, B. Wu, D. Qiu, and W. Hu, "Path planning for autonomous parallel parking based on piecewise Gauss pseudospectral method," *Automot. Eng.*, vol. 41, no. 12, pp. 1401–1409, 2019, doi: 10.19562/j.chinasae.qcgc.2019.012.008.

[7] H. Zhang, Y. Wang, J. Zheng, and J. Yu, "Path planning of industrial robot based on improved RRT algorithm in complex environments," *IEEE Access*, vol. 6, pp. 53296–53306, 2018, doi: 10.1109/ACCESS.2018.2871222.

[8] A. T. Khan, S. Li, S. Kadry, and Y. Nam, "Control framework for trajectory planning of soft manipulator using optimized RRT algorithm," *IEEE Access*, vol. 8, pp. 171730–171743, 2020.

[9] R. Cui, Y. Li, and W. Yan, "Mutual information-based multi-AUV path planning for scalar field sampling using multidimensional RRT*," *IEEE Trans. Syst., Man, Cybern., Syst.*, vol. 46, no. 7, pp. 993–1004, Jul. 2016, doi: 10.1109/TSMC.2015.2500027.

[10] J. Zhang, H. Chen, S. Song, and F. Hu, "Reinforcement learning-based motion planning for automatic parking system," *IEEE Access*, vol. 8, pp. 154485–154501, 2020, doi: 10.1109/ACCESS.2020.3017770.

[11] W. Liu, Z. Li, L. Li, and F.-Y. Wang, "Parking like a human: A direct trajectory planning solution," *IEEE Trans. Intell. Transp. Syst.*, vol. 18, no. 12, pp. 3388–3397, Dec. 2017, doi: 10.1109/TITS.2017.2687047.

[12] X. Chen and Y. Tian, "Learning to perform local rewriting for combinatorial optimization," in *Proc. 33rd Conf. Neural Inf. Process. Syst.*, Vancouver, BC, Canada, 2019, pp. 1–12.

[13] N. Ye, Y. Zhang, R. Wang, and R. Malekian, "Vehicle trajectory prediction based on hidden Markov model," *KSII Trans. Internet Inf.*, vol. 10, no. 7, pp. 3150–3170, 2016, doi: 10.3837/tiis.2016.07.016.

[14] B. Woosley and P. Dasgupta, "Integrated real-time task and motion planning for multiple robots under path and communication uncertainties," *Robotica*, vol. 36, no. 3, pp. 353–373, Nov. 2017, doi: 10.1017/S0263574717000443.

[15] F. Zhang, R. N. Dang, and K. Q. Li, "A fuzzy logic-based automatic parallel parking control scheme," *Automot. Eng.*, vol. 36, no. 9, pp. 1151–1156, 2014, doi: 10.19562/j.chinasae.qcgc.2014.09.023.

[16] Y. Q. Tu, H. Chen, and H. Y. Yang, "Autonomous parking method based on human-simulated intelligent control," *Control Eng. China*, vol. 21, no. 2, pp. 161–167, 2014, doi: 10.14107/j.cnki.kzgc.2014.02019.

[17] M. Mehndiratta, E. Kayacan, M. Reyhanoglu, and E. Kayacan, "Robust tracking control of aerial robots via a simple learning strategy-based feedback linearization," *IEEE Access*, vol. 8, pp. 1653–1669, 2020, doi: 10.1109/ACCESS.2019.2962512.

[18] K. Demirli and M. Khoshnejad, "Autonomous parallel parking of a car-like mobile robot by a neuro-fuzzy sensor-based controller," *Fuzzy Sets Syst.*, vol. 160, no. 19, pp. 2876–2891, Oct. 2009, doi: 10.1016/j.fss.2009.01.019.

[19] D. Xu, Y. Shi, and Z. Ji, "Model-free adaptive discrete-time integral sliding-mode-constrained-control for autonomous 4WMV parking systems," *IEEE Trans. Ind. Electron.*, vol. 65, no. 1, pp. 834–843, Jan. 2018, doi: 10.1109/TIE.2017.2739680.

[20] Q. Tian, Q. Cheng, H. Jing, Y. Yin, X. Zhang, and H. Liu, "Path tracking control strategy for off-road 4WS4WD vehicle based on robust model predictive control," *Robot. Auto. Syst.*, vol. 158, Dec. 2022, Art. no. 104267, doi: 10.1016/j.robot.2022.104267.

[21] J. Backman, T. Oksanen, and A. Visala, "Nonlinear model predictive trajectory control in tractor-trailer system for parallel guidance in agricultural field operations," *IFAC Proc. Volumes*, vol. 43, no. 26, pp. 133–138, 2010, doi: 10.3182/20101206-3-JP-3009.00023.

[22] Z. Hou, H. R. Dong, and S. Jin, "Model-free adaptive control with coordinates compensation for automatic car parking systems," *Acta Autom. Sinica*, vol. 41, no. 4, pp. 823–831, Apr. 2015, doi: 10.16383/j.aas.2015.c140026.

[23] W. Yan, J. Deng, and D. Xu, "Data-driven automatic parking constrained control for four-wheeled mobile vehicles," *Int. J. Adv. Robotic Syst.*, vol. 13, no. 6, Dec. 2016, Art. no. 172988141666366, doi: 10.1177/1729881416663667.

[24] Y. Xu, Z. Lu, S. Xin, W. Jia, B. Wei, and Y. Wang, "Study on an automatic parking method based on the sliding mode variable structure and fuzzy logical control," *Symmetry*, vol. 10, no. 10, p. 523, Oct. 2018, doi: 10.3390/sym10100523.

[25] J. K. Suhr and H. G. Jung, "Automatic parking space detection and tracking for underground and indoor environments," *IEEE Trans. Ind. Electron.*, vol. 63, no. 9, pp. 5687–5698, Sep. 2016, doi: 10.1109/TIE.2016.2558480.

[26] X. Jin, J. Yang, Y. Li, B. Zhu, J. Wang, and G. Yin, "Online estimation of inertial parameter for lightweight electric vehicle using dual unscented Kalman filter approach," *IET Intell. Transp. Syst.*, vol. 14, no. 5, pp. 412–422, May 2020, doi: 10.1049/iet-its.2019.0458.

[27] J. Meng and S. Song, "Parking path tracking method based on Kalman filter and fuzzy control," *Int. Core J. Eng.*, vol. 6, pp. 77–85, Jan. 2020, doi: 10.6919/ICJE.202001_6(1).0011.

[28] H. T. Yun, X. Zeng, and J. Z. Lin, "Vehicle emergency avoidance path tracking neural network auto disturbance rejection control," *Mech. Des. Manuf.*, no. 9, pp. 24–27 and 31, 2020, doi: 10.3969/j.issn.1001-3997.2020.09.007.

[29] E. Q. Zhao, G. F. Sun, and M. Y. Huang, "Modeling and simulation analysis of active disturbance rejection controller," *J. Qingdao Univ. Technol.*, vol. 42, no. 5, pp. 96–103, 2021, doi: 10.3969/j.issn.1673-4602.2021.05.014.

**MAOFEI ZHU** was born in Hefei, Anhui, China, in 1983. He received the Ph.D. degree in automotive engineering from the School of Automotive and Traffic Engineering, Hefei University of Technology, China, in 2011. He is currently an Assistant Professor with the School of Advanced Manufacturing Engineering, Hefei University, Hefei. He has authored or coauthored over 15 articles and holds 20 patents. His research interests mainly include vehicle system dynamics and control, intelligent vehicle control by wire, and advanced driver assistance systems.

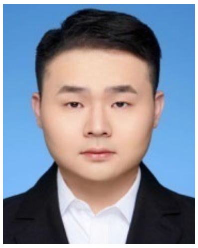

**QIAN LIU** was born in Hefei, Anhui, China, in 1996. He received the bachelor's degree in automotive engineering from Huainan Normal University, China, in 2020. He is currently pursuing the master's degree with the School of Advanced Manufacturing Engineering, Hefei University, Hefei. His research interests include automotive system dynamics and control, and active safety control system design.

**JIANWEN ZHOU** was born in Jianyang, Sichuan, China, in 1977. He received the master's degree from Northwestern Polytechnical University. He is currently a Professor in engineering with China Automotive Engineering Research Institute Company Ltd., Chongqing. His research interest includes the development and testing evaluation of automotive vehicle technology.

**WEI SHA** was born in 1982. He received the master's degree in automotive engineering from Jilin University. He is currently a Senior Engineer with China PUJIN Intelligent Technology (Anqing) Company Ltd., China. His research interest includes the development of automotive electronic control systems.

**RUNXIN NIU** was born in Hefei, Anhui, China, in 1971. He received the Ph.D. degree in automotive engineering from Jiangsu University, China, in 2007. He is currently a Researcher with the Hefei Institutes of Physical Science, Chinese Academy of Sciences. His research interest includes the development for path planning and control of unmanned driving systems.